

White-dwarf+main-sequence binaries identified from the tenth data release of Sloan Digital Sky Survey

Lifang Li^{1,2} ^{*}, Xiaobo Gong^{1,2,3}, Fenghui Zhang^{1,2}, Quanwang Han^{1,2,3}, and Xiaoyang Kong^{1,2,3}

¹Yunnan Observatories, Chinese Academy of Sciences, P.O.Box 110, Kunming, Yunnan Province 650011, China

²Key Laboratory for the Structure and Evolution of Celestial Objects, Chinese Academy of Sciences, P.O. Box 110, Kunming, Yunnan Province, 650011, China

³University of the Chinese Academy of Sciences, Beijing, 100049, China

Accepted yy mm dd. Received yy, mm, dd; in original form 2014 December 1

ABSTRACT

We have presented 309 new white-dwarf (WD) + main-sequence (MS) star binaries identified from the Sloan Digital Sky Survey (SDSS) Tenth Data Release (DR10). The majority of them consist of a white dwarf and a low-mass secondary (typically M dwarf) companion. The SDSS spectra of the newly found WDMS binaries with a DA/DB white dwarf and an M/late-K dwarf companion are analyzed based on a spectral decomposition/fitting method. White dwarf effective temperatures, surface gravities and masses together with the secondary star spectral types are obtained, and the stellar parameters of DA WDs with $T_{\text{eff}} \lesssim 14,000$ K are revised to the results in the case of 3D model atmosphere. Two independent distance estimates are derived from the flux-scaling factors between the WDMS SDSS spectra and the white dwarf and M-dwarf model spectra. It is found that about more than 20 per cent of the newly found WDMS binaries show a significant discrepancy between the two distance estimates. This might be caused by the effects of M-dwarf stellar activity or irradiation of the M dwarf companions by the white dwarf. The stellar parameter distributions are used to investigate the global properties of newly found WDMS binaries, the results shown in this work are consistent with those derived by previous investigators. Some WDMS binaries have been observed more than one (2–4) times by SDSS, it is found that four of them exhibit not only Hydrogen emission in all observable Balmer series lines in addition to He I line Balmer lines but also the rapid variation in the radial velocities of the components in these binaries. This suggests that they should be the post common envelope binaries (PCEBs) with a short orbital period. These young PCEBs are very important for limiting the results of common envelope phase of the binary evolution.

Key words: Stars: binaries: spectroscopic – stars: AGB and post-AGB – stars: evolution – stars: fundamental parameters

1 INTRODUCTION

White-dwarf + main-sequence (WDMS) binaries are very important celestial objects since they constitute a common final state objects of stellar evolution, a WD, and a MS star. They are the potential progenitors for most cataclysmic variables and perhaps type Ia supernova (SN Ia) and are therefore a subject which can inspire the keen interest of many investigators (Silvestri et al. 2006; Heller et al. 2009). The WDMS binaries are compact binaries containing a WD component whose progenitor star should have undergone a giant star (usually during red giant branch or a asymptotic gi-

ant branch) phase as a single star (Rebassa-Mansergas et al. 2010), the progenitor binaries of the WDMS binaries should be the wide initial ones. It is well known that the orbital separation of all types of close compact binaries, such as cataclysmic variables (CVs), X-ray binaries and double degenerate binaries are much shorter than the radius ($\sim 100R_{\odot}$) of a giant star (Maxted et al. 2009), implying that a large amount of angular momentum and orbital energy of their progenitor binaries have been lost by an unusual physical mechanism so called a common envelope (CE) evolution phase (Paczynski 1976; Webbink 1984, 2008; Iben & Tutukov 1986; Iben & Livio 1993). Up to now, the CE phase is believed to be a result of dynamically unstable mass transfer from a giant star to its MS companion

^{*} E-mail: llf@ynao.ac.cn

(Paczynski 1976; Webbink 1984; Hieblming 1989). At the beginning of the CE evolution, the secondary star starts a spiral-in process, then the CE is gradually ejected from the binary system owing to the friction induced by asynchronous rotation in CE. When the CE has been completely ejected from the system at the end of CE evolution, a post common envelope binary (PCEB), which consists of a compact object and a companion star, appears.

The CE evolution phase plays a central role in many evolutionary pathways leading to the formation of compact objects in the short period binary systems (Taam & Sandquist 2000; Taam & Ricker 2010), such X-ray binaries as natural laboratories for general relativity, CVs and double degenerate WD binaries as the potential progenitors of SN Ia, together with double degenerate neutron star binaries as the progenitors of short gamma-ray burst (Rebassa-Mansergas et al. 2012). Although the main features during the CE evolution phase have been depicted by Paczynski (1976) more than 30 years ago, and a lot of works on the formation theory of PCEBs have been carried out by various investigators (e.g. Iben & Livio 1993; Davis et al. 2008; Taam & Sandquist 2000; Postnov & Yungelson 2006; Politano et al. 2010), however, owing to the complex physical processes occurred in the CE phase and lack of the observational constraints, our understanding about CE phase is still very poor (Rebassa-Mansergas et al. 2007, 2012). Since the detached PCEBs have not been severely contaminated by mass transfer after they formed through a CE evolution, they are thought to be the most suitable objects for the constraints of the CE evolution result. That is to say, they are almost the real materials produced by the CE evolution except that the size of their orbit has been decreased by AM loss owing to magnetic stellar wind and/or gravitational wave radiation. Among all PCEBs, those composed of a WD and a MS star represent the most promising population for deriving such observational constraints, as they are essentially most common population of PCEBs and their physical parameters can be derived from observations through 2-8m telescopes (Nebot Gómez-Morán et al. 2011).

One of the many interesting by-products of the Sloan Digital Sky Survey (SDSS; York et al. 2000; Stoughton et al. 2002; Adelman-McCarthy et al. 2008; Abazajian et al. 2009) is the identification of a large number of unresolved, close binary systems. In particular, the five-color (u, g, r, i photometry and z) and spectra covering almost the entire optical wavelength range permit to easy identification of binaries contained a blue white dwarf (blue) and a red low-mass M dwarf secondary (Silvestri et al. 2006). Therefore, the SDSS has been thought to be very efficient in searching for WDMS binaries. Up to now, more than 2,500 WDMS binaries have been discovered in SDSS survey (Silvestri et al. 2006, 2007; Adelman-McCarthy et al. 2007; Heller et al. 2009; Liu et al. 2012; Rebassa-Mansergas et al. 2012, 2013; Li et al. 2014) since Raymond et al. (2003) and Schreiber & Gänsicke (2003) first attempted to investigate the WDMS binaries in the SDSS, however the orbital periods of only about 200 WDMS binaries have been determined by the various investigators through the radial velocity observations, and is clearly very insufficient to limit the results of the CE evolution. This suggests that the orbital periods of most WDMS binaries are difficultly determined by observations due to insufficient telescope time for their radial

velocity observations. Therefore, it is necessary to find more WDMS binaries from the new data released by SDSS or by other spectral survey telescope, such as LAMOST (also called GuoShouJing Telescope, Ren et al. 2013; Wei et al. 2012).

In this work, we present 309 new WDMS binaries, which are mainly composed of a white dwarf and an M dwarf, newly identified from SDSS (DR10) based on a color-selection criteria (Li et al. 2014) originally developed by Liu et al. (2012) and a criteria developed by Gong et al. (2014, in preparation). We have analyzed their SDSS spectra by using a method proposed by Heller et al. (2009), then derived the fundamental physical parameters for the two spectral components in each WDMS binary which are composed of a DA/DB white dwarf and an M-dwarf. At last, based on the stellar parameter distributions, the general properties of the WDMS binaries identified from SDSS by us are discussed.

2 WDMS BINARIES IDENTIFIED FROM SDSS DR10

Based on a color-selection criteria (Li et al. 2014) originally developed by Liu et al. (2012) and a color-selection criteria for searching for WD stars from LAMOST and SDSS (Gong et al. 2014, in preparation), we identified 2198 WDMS binaries from SDSS DR10, and 1889 WDMS binaries of them had been identified by the previous investigators (Silvestri et al. 2007; Heller et al. 2009; Liu et al. 2012; Wei et al. 2012; Rebassa-Mansergas et al. 2013; Li et al. 2014). Therefore, 309 new WDMS binaries are identified from SDSS DR10. In these new binaries, 220 binary systems contain a DA WD component, 32 systems contain a DB WD component, and 57 systems contain a WD component with the other spectral types or an unknown spectral type because of a low SN. The infrared counterparts of some new WDMS binaries are obtained by cross-match (in a radius of 5 arc-seconds) with the Two Micron All Sky Survey (2MASS: Skrutskie et al. 2006), the UKIRT Infrared Sky Survey (UKIDSS: Dye et al. 2006; Lawrence et al. 2007; Warren et al. 2007), and the Wide-field Infrared Survey Explorer (WISE: Wright et al. 2010). The object name, coordinates (in degrees) and SDSS $ugriz$, UKIDSS $yjhz$, 2MASS JHK and WISE w_1, w_2 magnitudes of 311 new WDMS binaries are listed in Table 1.

3 STELLAR PARAMETERS

3.1 Stellar parameters of new WDMS binaries containing a DA/DB WD companion

Based on a method, which can remove a mutual dependence of the scaling factors and the effects of identifying a local χ^2 minimum, proposed by Heller et al. (2009), we decomposed/fitted the observed spectra of the new WDMS binaries (with a DA/DB WD component) identified from SDSS DR10. In the course of the fitting of their spectra, the theoretical spectral grid of the DA WDs is the same as Liu et al. (2012) and Li et al. (2014) who employed a theoretical spectral grid developed by Koester (2010). In order to obtain the stellar parameters of some WDMS binaries with a DB WD star component, we employ a theoretical spectral

grid of DB WDs also developed by Koester (2010), in which the surface gravity, $\log g_{\text{WD}}$, covers a range from 7.0 to 9.0 in steps of 0.25, and the effective temperature, T_{WD} , covers a range from 8,000 K to 40,000 K, in steps of 500 K for $T_{\text{eff}}^{\text{WD}} \lesssim 10,000$ K, 1,000 K for $10,000 \text{ K} \lesssim T_{\text{eff}}^{\text{WD}} \lesssim 20,000$ K, and 2,000 K for $T_{\text{eff}}^{\text{WD}} \gtrsim 20,000$ K. With the help of these theoretical spectral grids, we can obtain the surface gravity and effective temperature of DA/DB WDs in WDMS binaries identified from SDSS DR10. The parameter spaces of the surface gravity and effective temperature for the M dwarfs are the same as those used in Li et al. (2014). Since the determination of the M dwarf metallicity is easily affected by the signal-to-noise ratio (SN) of the observed spectra of the WDMS binaries which should be in the neighborhood of the sun (Li et al. 2014), the metallicity of the M dwarfs is set to be the solar abundance, i.e. $[\text{Fe}/\text{H}] = 0$, in this work, then the template spectra can be produced by the second version of BaSeL standard library (Lejeune et al. 1997, 1998). In addition, a few new WDMS binaries found from SDSS DR10 with a K-dwarf star companion. In the course of the spectral fitting of these WDMS binaries, the parameter spaces of the effective temperature, surface gravity, mass and radius of the K-dwarf stars are produced according to the theoretical models given by (Baraffe et al. 1998). The template spectra for K dwarfs are also given by the BaSeL standard library. On the basis of the best fitting result of the observed spectrum, we can obtain the effective temperature and surface gravity of the MS star companion in each WDMS binary. The results of the spectral analysis of three typical WDMS binaries [SDSS J163033.26+393714.0 (containing a DA WD star and an M dwarf companion), SDSS J111615.65+251716.1 (containing a DA WD star and a K-type star companion) and SDSS J103334.76+131159.6 (containing a DB WD star and an M dwarf companion)] are shown in Fig. 1. The effective temperature and surface gravity determined for the two components in WDMS binaries through spectral analysis are presented in Table 2.

Based on the spectral type of the M dwarf and the empirical relations of $Sp - M$ and $Sp - R$ (Rebassa-Mansergas et al. 2007), the mass and the radius of the M dwarf in each WDMS binary can be derived. For the WDs in WDMS binaries, their parameters $T_{\text{eff}}^{\text{WD}}$ and $\log g_{\text{WD}}$ are determined from the best spectral fitting based on results of a 1D model atmosphere (Koester 2010) at first, then they are revised to the results of a 3D model atmosphere (Tremblay et al. 2013) for DA WDs with $T_{\text{eff}} \lesssim 1,4000$ K. The masses of the WDs can be determined according to the newly updated cooling models for DA/DB WDs in Bergeron, Wesemel & Beauchamp (1995), and their radii can be obtained through a recent mass-radius relation presented in Holberg, Oswalt & Barstow (2012). In order to determine the cooling age of the WD components in the WDMS binaries, we have made a distinction between WD stars with a He-core and WD stars with a CO-core on the basis of their masses derived from the spectral analysis as Li et al. (2014) at first. The WD stars with $M_{\text{WD}} \gtrsim 0.5M_{\odot}$ are defined to be the CO WDs and the others are regarded as He WDs, although we cannot conform that which type of WD with $M_{\text{WD}} \sim 0.48 - 0.51M_{\odot}$ is most probable (Hurley, Pols & Tout 2002; Zorotovic, Schreiber & Gänsicke 2011). The cooling age of the He WDs is estimated by interpolating cooling mod-

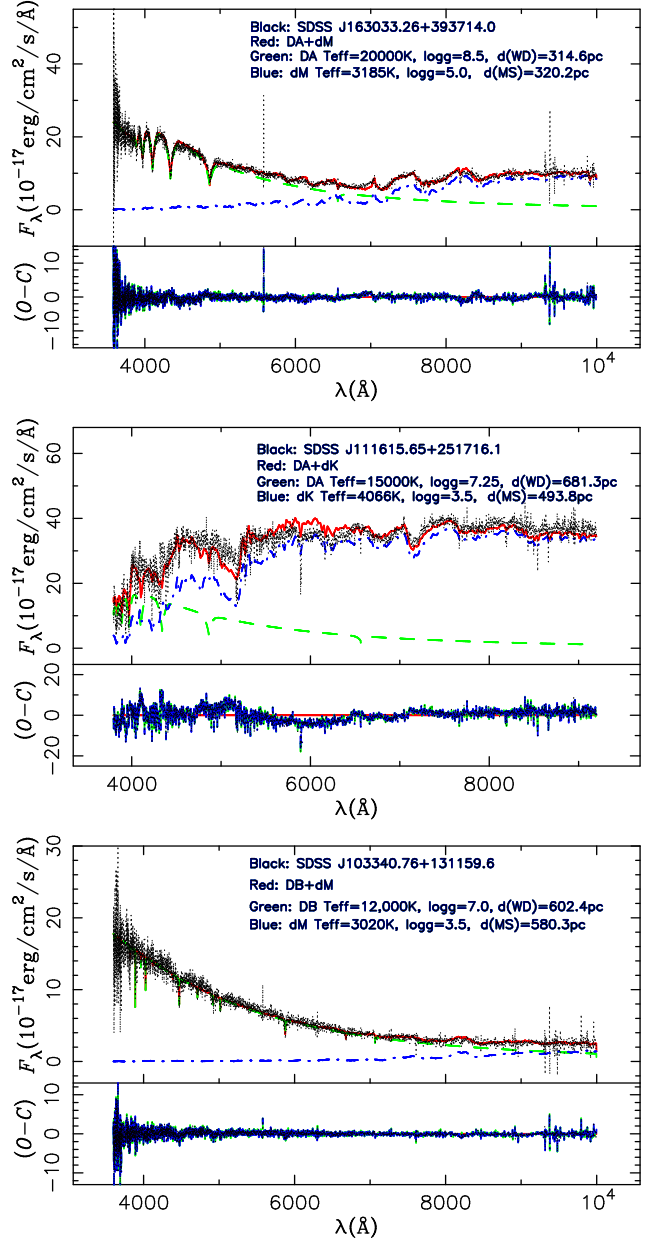


Figure 1. Two-component fit to the spectra of the SDSS WDMS binaries. Shown are examples for objects (DA+dM: SDSS J163033.26+393714.0, DA+dK: SDSS J111615.65+251716.1, and DB+dM: SDSS J103334.76+131159.6). In each panel, the dotted line corresponds to the observed flux, the dashed line represents the WD model flux, the dot-dashed line represents the main sequence star model flux, and the solid line represents the total DA+MS model flux. $O - C$ represents the residuals between the observation flux and model flux.

els of Althaus & Benvenuto (1997), and the cooling age of the CO WDs is estimated through a interpolation method according to the cooling models of an updated version of Bergeron, Wesemel & Beauchamp (1995). The values of these stellar parameters derived from the results of the best spectral fitting are also listed in Table 2.

As Li et al. (2014), the two independent distances for the WD and M-dwarf companions in WDMS binaries from

the earth are estimated on the basis of the best-fitting flux scales [a and b as described in Liu et al. (2012) and Heller et al. (2009)] by the following equations,

$$d_{\text{WD}}[\text{pc}] = \frac{R_{\text{WD}}[R_{\odot}]}{1\text{pc}} \sqrt{\frac{\pi}{a}}, \quad (1)$$

and

$$d_{\text{M}}[\text{pc}] = \frac{R_{\text{M}}[R_{\odot}]}{1\text{pc}} \sqrt{\frac{\pi}{b}}, \quad (2)$$

where R_{M} is the radii of the MS components in WDMS binaries, d_{M} is the distance of the MS components from the earth, and the meaning of the other physical quantities in eqs. (1) and (2) is the same as that described in Li et al. (2014), then a parameter C used to describe the difference between d_{WD} and d_{M} proposed by Heller et al. (2009) is written as the following:

$$C = \sqrt{2} \frac{d_{\text{WD}} - d_{\text{M}}}{d_{\text{WD}} + d_{\text{M}}}, \quad (3)$$

two independent distances for the WD and M dwarf from the Earth, together with the parameter C , are also presented in Table 2.

3.2 Distributions of stellar parameters of new WDMS binaries

The stellar parameters of 205 new WDMS binaries with a DA WD component and 32 new WDMS binaries with a DB WD component identified from SDSS DR10 have been determined in Section 3.1. Their global properties of the WDMS binaries are investigated here. Fig. 2 shows the distributions of the mass M_{WD} , surface gravity $\log g_{\text{WD}}$ and effective temperature T_{WD} of the DA/DB white dwarfs in 396 WDMS binaries [also including 143 DA+MS binaries and 16 DB+MS binaries found from SDSS DR9 by Li et al. (2014), solid line] and in 253 WDMS binaries with a DA/DB WD component (the stellar parameters derived in this work, shaded zone). As seen from the bottom panel of Fig. 2, the effective temperature of the white dwarfs in most WDMS binaries is located in a region between 6,000 K and 25,000 K, only about 25 per cent of the white dwarfs in WDMS binaries have an effective temperature higher than 25,000 K in both cases. This should be caused by a rapid cooling velocity for the white dwarfs with a relatively high effective temperature (Li et al. 2014). Meanwhile, it is found in the intermediate panels of Fig. 2 that an average surface gravity of the WDs is of about 10^8 cm/s^2 and the surface gravitation of most WDs is larger than 7.75. These results are consistent with those derived by Liu et al. (2012). From the top panel of Fig. 2, we can find that the mass of WDs in WDMS binaries peaks at $\sim 0.5 M_{\odot}$, and the average mass is of $0.632 M_{\odot}$ and $0.692 M_{\odot}$ for the DA/DB WDs in new WDMS binaries and in all WDMS binaries, respectively. This is in good agreement with the results derived by the previous investigators (e.g. Kepler 2014; Rebassa-Mansergas et al. 2007, 2012).

The cooling age of the DA/DB WD components in our identified WDMS binaries has been estimated by interpolation based on the cooling models of He WDs (Althaus & Benvenuto 1997) and CO WDs (Bergeron, Wesemmel & Beauchamp 1995). The cooling age

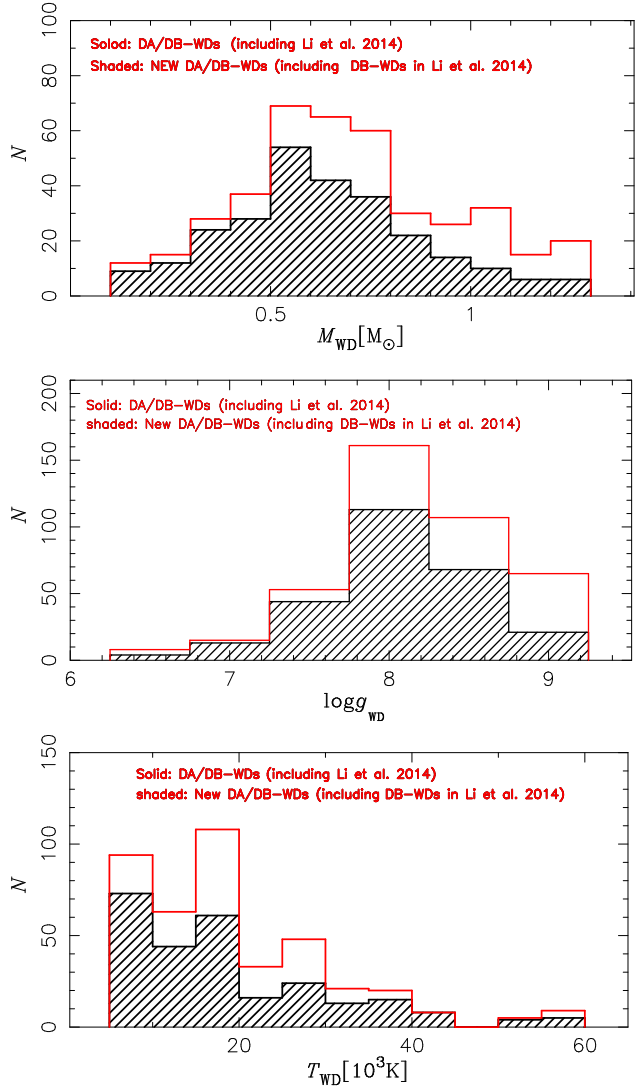


Figure 2. White dwarf mass, $\log g_{\text{WD}}$ and effective temperature distributions obtained from WDMS binaries identified from SDSS. Solid line represents the parameter distributions of all DA/DB-WDs identified by us from DR9 and DR10, and the shaded zone represents the new DA/DB-WDs in the WDMS binaries newly found from DR10 and in the WDMS binaries containing a DB WD component found by Li et al. (2014).

estimates of the white dwarfs in our WDMS binary sample identified from SDSS DR9 and DR10 are shown in Fig. 3. The cooling tracks of CO WD models with different masses (0.5, 0.6, 0.7, 0.8, 0.9, 1.0, 1.1 and 1.2 M_{\odot} , respectively), together with the estimates of cooling ages of only CO white dwarfs, are shown in the top panel of Fig. 3. The bottom panel of Fig. 3 shows the cooling age distributions of DA/DB WDs (solid line) in 396 WDMS binaries found by us and in new WDMS binaries, together with 16 WDMS binaries found by us from SDSS DR9 (shaded zone), respectively. As seen from the bottom panel of Fig. 3, the cooling age of the WDs in our WDMS binaries covers a region from 10^5 to 10^{10} yrs in both cases, and the cooling age of the majority of DA/DB white dwarfs is larger than 10^8 yrs. In addition, the average cooling age of the WDs in our WDMS sample is of about 2.0×10^8 yrs. This suggests that the young DA white

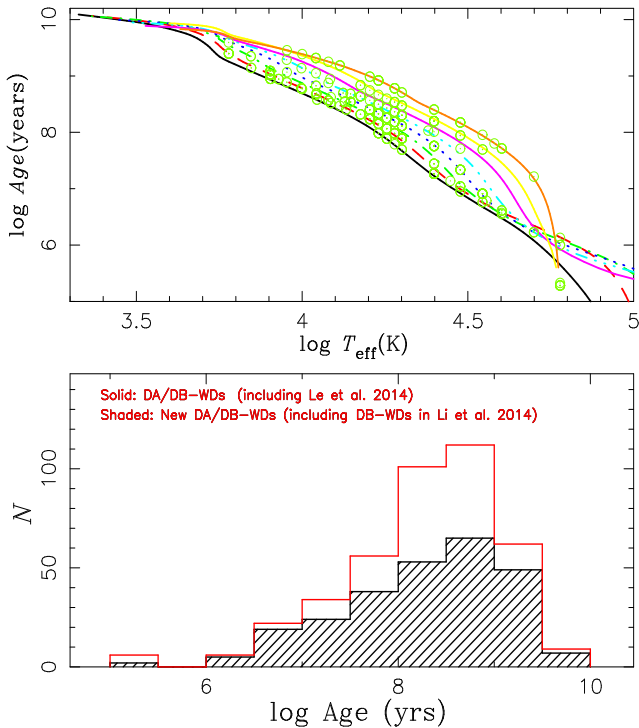


Figure 3. Top panel: The determination of the cooling age of CO white dwarfs in WDMS binaries newly identified from SDSS DR10. The lines represent the cooling models ($M_{\text{WD}} = 0.5, 0.6, \dots, 1.2 M_{\odot}$) of Bergeron, Wesemmel & Beauchamp (1995), the symbol \odot represents the observations. Bottom panel: The solid line represents the distribution of the cooling ages of DA/DB-WDs in all WDMS binaries found from DR9 and DR10, and the shaded zone denotes that in those newly identified from SDSS DR10 and the WDMS binaries containing a DB WDs found by Li et al. (2014).

dwarfs is very rare. This is also a result of the rapid cooling velocity of the white dwarfs with a high effective temperature. This is consistent with the result that the effective temperature of most WDs are between 6,000 and 25,000K as shown in Fig. 2.

On the basis of the best fittings to their SDSS observed spectra, the effective temperature and the surface gravity of the M stars in our identified WDMS binary sample have been obtained. We can derive the spectral type of the M dwarf in each WDMS binary according to an empirical $\text{Sp} - T_{\text{eff}}$ relation proposed by Rebassa-Mansergas et al. (2007). The distribution of the M dwarf spectral types in our WDMS binary sample (including a DA/DB WD component) is displayed in Fig. 4, in which the solid line represents the all DA/DB WDs in WDMS binaries identified by us from SDSS DR9 and DR10 and the shaded zone represents the new DA/DB WDs in WDMS binaries found from DR10, together with the DB WDs in WDMS binaries found by us from SDSS DR9. It is found in Fig. 4 that the spectral types of the majority of M dwarf components in WDMS binaries are located in a region from M3 to M6 in both cases. This is similar to the results found by Heller et al. (2009); Liu et al. (2012) and Rebassa-Mansergas et al. (2007, 2012, 2013).

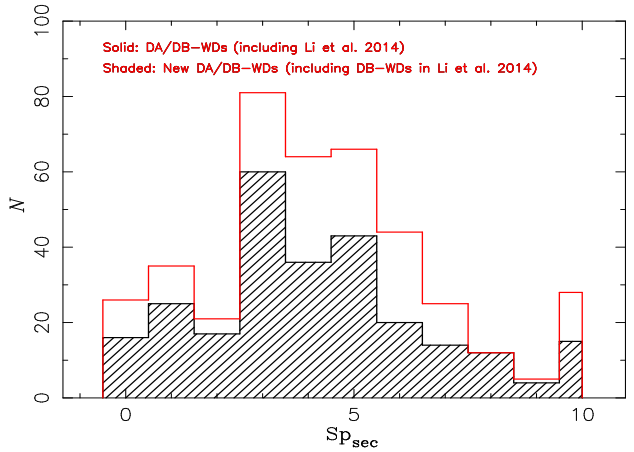


Figure 4. The distributions of the spectral types of the M Dwarfs in WDMS binaries with a DA or DB WD component found from SDSS. Solid line represents the spectral type distribution of M dwarfs in all WDMS binaries, and the shaded zone represents that of M dwarfs in WDMS binaries newly identified from DR10, together with DB+dM binaries found by Li et al. (2014).

3.3 WDMS binaries with several SDSS spectra

In this work, we have identified 121 WDMS binaries with several SDSS spectra observed in different times. They are listed in Table 3. Two (SDSS J220451.62+113230.8 and SDSS J111544.56+425822.4) of these WDMS binaries are newly identified by us from SDSS DR10, their spectra are displayed in Fig. 5 and Fig. 6, respectively. As seen from Fig. 5, SDSS J220451.62+113230.8 have been observed three times by SDSS spectral survey, however its spectra observed in different times do not show any obvious variation in the radial velocities of its two components. This suggests that it might be a PCEB with a low orbital inclination or it is a WDMS binary with a wide separation and a long orbital period so that the variation in its radial velocity can not be found by us in a short period. Meanwhile, one (SDSS J095043.96+391541.7) of these WDMS binaries was found by us from SDSS DR9 (Li et al. 2014), its spectra are shown in the top panel of Fig. 6. Another two WDMS binaries [SDSS J131751.72+673158.4 and SDSS J142947.62-010606.9 listed in Rebassa-Mansergas et al. (2013) and Silvestri et al. (2006), respectively] are also plotted in Fig. 6 since their spectra shows the same properties as those of SDSS J111544.56+425822.4 and SDSS J095043.96+391541.7 recently identified from SDSS by us.

It is found in Fig. 6 that the SDSS observed spectra of four WDMS binaries (SDSS J095043.96+391541.7, SDSS J111544.56+425822.4, SDSS J143947.62-010606.9, and SDSS J131751.72+673158.4) share a similar characteristics, i.e. their SDSS spectra exhibit Hydrogen emission in all observable Balmer series lines in addition to He I emission. This phenomenon was primarily found in SDSS J143947.62-010606.9 by Silvestri et al. (2006), who suggest this is caused by the photoionization and recombination induced by irradiation of the M dwarfs in these WDMS binaries rather than the mass accretion as that in CVs, since the emission line width ($\lesssim 20$ angstroms) in these WDMS binaries is much narrower than that ($\sim 30 - 40$ angstroms) in CVs. As seen from Fig. 6, the WDs in such WDMS binaries usually have

Table 1. Object name, coordinates (in degrees), and SDSS *ugriz*, 2MASS *JHK*, UKIDSS *yjkh* and WISE *w1,2* magnitudes of the 468 WDMS binaries identified from SDSS DR9 and DR10. The complete table is available in the electronic edition of the paper.

| SDSS J | RA | DEC | u | g | r | i | z | J | H | K | y | j | h | k | w1 | w2 |
|--------------------|----------|----------|-------|-------|-------|-------|-------|-------|-------|-------|-------|-------|-------|-------|-------|-------|
| 000756.04+055723.5 | 1.98349 | 5.95653 | 21.05 | 20.52 | 20.50 | 20.04 | 19.49 | — | — | — | 18.65 | 18.21 | — | — | 16.80 | 16.62 |
| 001707.14+040145.3 | 4.27974 | 4.02926 | 21.65 | 21.02 | 21.15 | 20.71 | 20.31 | — | — | — | 19.34 | 18.77 | 18.25 | 17.81 | 17.65 | 16.46 |
| 001744.95+001203.6 | 4.43731 | 0.20100 | 20.40 | 19.92 | 20.08 | 20.63 | 19.35 | 13.97 | 13.38 | 13.14 | 14.42 | 13.98 | — | 13.15 | 13.03 | 12.99 |
| 002438.47+024024.7 | 6.16029 | -2.67352 | 21.47 | 20.89 | 20.79 | 20.20 | 19.54 | — | — | — | — | — | — | — | 17.07 | 16.57 |
| 003509.76+023153.5 | 8.79068 | 2.53153 | 21.43 | 20.93 | 21.10 | 20.94 | 20.43 | — | — | — | 19.54 | 19.27 | 18.60 | 18.28 | — | — |
| 003830.93+081457.2 | 9.62887 | 8.24921 | 21.00 | 20.60 | 20.53 | 20.49 | 20.20 | — | — | — | 20.01 | — | — | — | 16.51 | 16.23 |
| 003955.54+104702.9 | 9.98143 | 10.78413 | 20.72 | 20.26 | 20.36 | 20.15 | 19.77 | — | — | — | — | — | — | — | — | — |
| 004212.74+004220.6 | 10.55310 | 0.70573 | 21.45 | 20.94 | 20.72 | 19.78 | 19.03 | — | — | — | — | — | 17.31 | 17.08 | 16.87 | 16.72 |
| 004435.57+000036.7 | 11.14822 | -0.01020 | 19.13 | 17.68 | 16.69 | 16.22 | 15.94 | 14.78 | 14.13 | 14.01 | — | — | — | — | 13.99 | 13.96 |
| 004643.54+084227.5 | 11.68143 | 8.70763 | 19.48 | 19.37 | 19.48 | 19.40 | 19.02 | — | — | — | 18.14 | 17.59 | 16.95 | 16.68 | 16.49 | 15.95 |
| 004827.34+075939.8 | 12.11392 | 7.99438 | 19.47 | 19.31 | 19.39 | 18.73 | 18.10 | 16.88 | 15.81 | 15.67 | 17.25 | 16.72 | 16.25 | 16.01 | 15.85 | 15.71 |
| 005308.36+085631.6 | 13.28483 | 8.94212 | 21.58 | 21.00 | 20.80 | 20.25 | 19.52 | — | — | — | 18.75 | 18.07 | 17.78 | 17.46 | 17.45 | 16.38 |
| 005443.84+070921.2 | 13.68265 | 7.15590 | 18.20 | 18.41 | 18.72 | 18.83 | 19.59 | 16.78 | 15.79 | 17.11 | 17.34 | 16.77 | 16.20 | 15.95 | 15.70 | 15.50 |
| 005752.57+035851.6 | 14.46905 | 3.98101 | 20.85 | 20.42 | 20.58 | 20.36 | 19.99 | — | — | — | 19.15 | 18.73 | 18.19 | 17.88 | — | — |
| 005827.26+005642.6 | 14.61359 | 0.94516 | 23.04 | 21.21 | 19.96 | 18.50 | 17.56 | 16.04 | 15.75 | 14.97 | — | 16.08 | 15.51 | 15.23 | 14.77 | 14.56 |
| 005906.65+003802.2 | 14.77772 | -0.63394 | 21.98 | 20.72 | 19.61 | 18.25 | 17.38 | 16.00 | 15.64 | 15.00 | — | — | — | — | 14.97 | 14.73 |
| 010055.32+074758.9 | 15.23052 | 7.79970 | 19.23 | 18.98 | 19.21 | 19.07 | 18.65 | — | — | — | 17.76 | 17.22 | 16.73 | 16.42 | — | — |

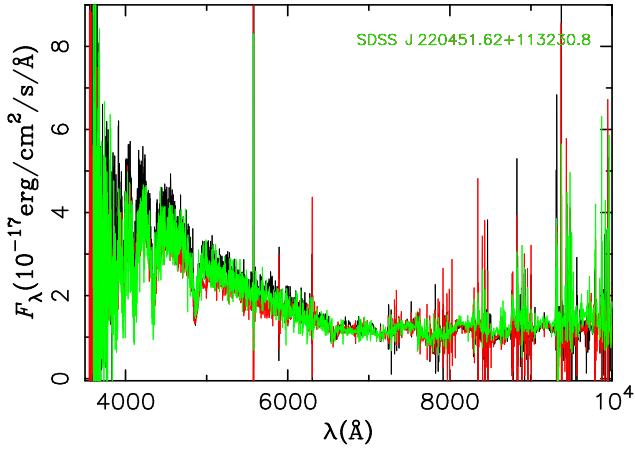


Figure 5. Shown is the spectra of a new WDMs binary with three different SDSS spectra.

a very high effective temperature based on their spectral profile, and therefore they are very young WD stars. In addition, it is found from the sub-plot in the upper right corner of each panel of Fig. 6 that the components in three binaries exhibit spectral line shift. In particular for SDSS J131751.72+673158.4, its two SDSS spectra span an interval of only one day (i.e. MJD55622 and MJD55623). This suggests that such WDMs binaries should be the young PCEBs with a short period. Although SDSS J143947.62-010606.0 does not show any variation in the radial velocity of its WD component, it might be the very young short-period PCEBs with a very low inclination. We would obtain the orbital periods on the basis of their radial velocity observations in the future.

3.4 Distance distribution for WDMs binaries

As mentioned sect. 3.1, the two independent distance estimates for each DA/DB WD and its M dwarf companion from the earth have determined according to the flux scale factors obtained from the best fitting the SDSS observed spectra of WDMs binaries. We compare the distances of the white dwarfs with those of their M-dwarf companions in Fig. 7. In Fig. 7, the symbol pluses represent 396 analyzed WDMs binaries identified from SDSS DR9 and DR10, the solid dots represent the new WDMs binaries identified from DR10, together with those containing a DB WD component which the

physical parameters are newly derived in this work, the solid line denotes the case with $d_{WD} = d_M$, the two dashed lines span a tolerance fan for $C = 0.5$ as Li et al. (2014). As seen from Fig. 7 and Table 2, about 80 percent of the WDMs binaries with a distance discrepancy coefficient C (Heller et al. 2009) determined base on Eq. (3) are in a range between -0.5 and 0.5 in both cases. This suggests that about 80 percent of the WDMs binaries with a DA/DB white dwarf component have $d_{WD} \simeq d_{sec}$, implying that about 20 per cent of these binary systems show a significant difference between the two distance estimates for the WDs and M-dwarfs. This is similar to the results derived by Rebassa-Mansergas et al. (2007), Heller et al. (2009), Liu et al. (2012) and Li et al. (2014).

4 DISCUSSION AND CONCLUSION

In this work, we have identified 2198 new WDMs binaries from SDSS DR10 based on a color-selection criteria (Li et al. 2014) and a color-selection criteria for searching WDs from SDSS or LAMOST (Gong et al. 2014, in preparation). 1889 of which have been discovered by previous investigators (e.g. Raymond et al. 2003; Silvestri et al. 2007; Heller et al. 2009; Rebassa-Mansergas et al. 2013; Liu et al. 2012; Li et al. 2014). Therefore, 309 WDMs binaries are newly identified by us from DR10, these binaries include 220 DA+MS binaries, 32 DB+MS binaries, and 57 WDMs binaries containing a WD component with the other spectral types of WDs. Kepler (2014) reports 180 WDMs binaries identified from SDSS DR10, 120 of which have been discovered by Li et al. (2014) and Rebassa-Mansergas et al. (2013). Therefore, about 60 WDMs binaries recently found by Kepler (2014) are probably in 309 WDMs binaries discovered by us independently.

Based on a χ^2 minimization technique originally developed by Heller et al. (2009) and Rebassa-Mansergas et al. (2007), we have determined the independent stellar parameters (effective temperature, surface gravitation, mass, radius and distance) of the two components in 237 new WDMs binaries with a DA/DB WD component. The other 15 new WDMs binaries with a DA WD component have a very low SN, the stellar parameters for their components cannot be precisely determined in this work. The fraction of the WDs with a mass larger than $\sim 0.9M_{\odot}$ in Li et al. (2014) is slightly higher than those in the previous investigators' works (e.g. Silvestri et al. 2006; Rebassa-Mansergas et al.

Table 2. Stellar parameters for 468 WDMS binaries identified from SDSS DR9 and DR10. The complete table is available in the electronic edition of the paper.

| SDSS J | Type | PLT | MJD | FIB | $T_{\text{eff}}^{\text{WD}}$ (K) | $\log g_{\text{WD}}$ (cm/s^2) | $T_{\text{eff}}^{\text{sec}}$ (K) | $\log g_{\text{sec}}$ (cm/s^2) | d_{WD} (pc) | M_{WD} (M_{\odot}) | r_{WD} (R_{\odot}) | d_{M} (pc) | M_{sec} (M_{\odot}) | r_{sec} (R_{\odot}) | C | $\log \text{Age}$ (yrs) |
|--------------------|-------|------|-------|-----|-------------------------------------|---|--------------------------------------|--|-------------------------|------------------------------------|------------------------------------|------------------------|-------------------------------------|-------------------------------------|-------|----------------------------|
| 000756.04+055723.5 | DA+dM | 4416 | 55828 | 502 | 18000 | 8.250 | 3020 | 4.0 | 771.11 | 0.778 | 0.011 | 577.95 | 0.26 | 0.26 | 0.20 | 8.25 |
| 001707.14+040145.3 | DA+dM | 4299 | 55827 | 686 | — | — | — | — | — | — | — | — | — | — | — | — |
| 001744.95+001203.6 | DA/dM | 4219 | 55480 | 618 | 17000 | 8.000 | 3843 | 5.0 | 653.36 | 0.620 | 0.013 | 732.35 | 0.47 | 0.49 | -0.08 | 8.15 |
| 002438.48-024024.7 | DA/dM | 4367 | 55566 | 278 | 19000 | 8.250 | 3020 | 4.0 | 1027.19 | 0.780 | 0.011 | 620.68 | 0.26 | 0.26 | 0.35 | 8.18 |
| 003509.76+023153.5 | DA/dM | 4304 | 55506 | 520 | 25000 | 8.750 | 2281.0 | 3.5 | 899.07 | 1.073 | 0.007 | 147.75 | 0.13 | 0.12 | 1.01 | 8.20 |
| 003830.93+081457.2 | DA/dM | 4542 | 55833 | 444 | 25000 | 7.750 | 3843 | 5.5 | 1643.46 | 0.529 | 0.016 | 2554.01 | 0.47 | 0.49 | -0.31 | 7.27 |
| 003955.54+104702.9 | DA/dM | 5656 | 55940 | 110 | 18000 | 8.250 | 2856 | 3.5 | 688.67 | 0.778 | 0.011 | 522.33 | 0.20 | 0.20 | 0.19 | 8.25 |
| 004212.74+004220.6 | DA/dM | 3589 | 55186 | 680 | 25000 | 8.750 | 3185 | 4.5 | 904.01 | 1.073 | 0.007 | 504.30 | 0.32 | 0.33 | 0.40 | 8.20 |
| 004435.57-000036.7 | WD/dM | 3588 | 55184 | 34 | — | — | — | — | — | — | — | — | — | — | — | — |
| 004643.54+084227.5 | DB/dM | 4544 | 55855 | 458 | 8500 | 7.000 | 3020 | 3.5 | 464.75 | 0.189 | 0.023 | 370.18 | 0.26 | 0.26 | 0.16 | 8.71 |
| 004827.34+075939.8 | DA/dM | 4543 | 55888 | 890 | 25000 | 8.250 | 3185 | 5.0 | 614.92 | 0.792 | 0.011 | 335.26 | 0.32 | 0.33 | 0.42 | 7.76 |
| 005308.36+085631.6 | DA+dM | 4546 | 55835 | 590 | — | — | — | — | — | — | — | — | — | — | — | — |
| 005443.84+070921.2 | DA/dM | 4546 | 55835 | 304 | 25000 | 8.250 | 3843 | 5.5 | 434.82 | 0.792 | 0.011 | 1201.24 | 0.47 | 0.49 | -0.66 | 7.76 |
| 005752.57+035851.6 | DA/dM | 4307 | 55531 | 858 | 25000 | 9.000 | 3185 | 4.0 | 499.27 | 1.203 | 0.006 | 749.06 | 0.32 | 0.33 | -0.28 | 8.40 |
| 010055.32+074758.9 | DA/dM | 4546 | 55835 | 996 | 19000 | 8.250 | 3185 | 4.5 | 383.30 | 0.780 | 0.011 | 445.49 | 0.32 | 0.33 | -0.11 | 8.18 |

Notes in Table 2: (1) L: WDMS binaries identified by Li (2014); (2) N: New WDMS binaries identified from DR10

Table 3. Object name, coordinates (in degrees), plates, MJD, and Fibres of 121 WDMS binaries observed by SDSS several times. The complete table is available in the electronic edition of the paper.

| SDSS J | RA | DEC | PL-MJD-Fib | PL-MJD-Fib | PL-MJD-Fib | PL-MJD-Fib |
|----------------------|----------|----------|-----------------|-----------------|-----------------|-----------------|
| 001749.25 – 000955.4 | 4.45519 | -0.16539 | 0389-51795-0112 | 0687-52518-0109 | 4218-55479-0064 | |
| 002801.68+002137.7 | 7.00701 | 0.36047 | 0689-52262-0424 | 3586-55181-0570 | | |
| 003628.07 – 003125.0 | 9.11695 | -0.52360 | 0690-52261-0222 | 3586-55181-0072 | 0689-52262-0022 | |
| 005457.61 – 002517.2 | 13.74004 | -0.42145 | 0394-51913-0110 | 4224-55481-0228 | 0394-51812-0118 | 0394-51876-0109 |
| 010345.56+003746.7 | 15.93985 | 0.62965 | 1498-52914-0466 | 3735-55209-0723 | 1083-52520-0638 | 1497-52886-0615 |
| 012259.56+154253.9 | 20.74817 | 15.71496 | 0424-51893-0404 | 5140-55836-0604 | | |
| 014745.03 – 004911.1 | 26.93761 | -0.81976 | 0699-52202-0094 | 3606-55182-0484 | | |
| 015225.39 – 005808.6 | 28.10579 | -0.96906 | 1504-52940-0083 | 3606-55182-0294 | | |
| 023435.58 – 004818.4 | 38.64824 | -0.80512 | 0706-52199-0296 | 3745-55234-0340 | 0705-52200-0017 | |
| 023804.40 – 000545.7 | 39.51831 | -0.09602 | 0706-52199-0190 | 3745-55234-0200 | | |
| 024505.48+002804.6 | 41.27282 | 0.46794 | 0707-52177-0471 | 3651-55247-0805 | | |
| 025123.34 – 011314.4 | 42.84724 | -1.22068 | 0708-52175-0243 | 4241-55450-0124 | | |

2007, 2013). One possible explanation for this behaviour is that the SN of the observed spectra has a significant influence on the determination of the metallicity of the M dwarfs and the surface gravity of two components, and maybe on the determination of the masses of the WD stars in WDMS binaries. We analyze the spectra of these WDMS binaries again based on an assumption that the metallicity of the M dwarfs in these binaries is the solar one. In fact, all of these binaries are in the neighborhood of the sun, and the atmosphere of the M dwarfs in WDMS binaries should not be seriously polluted by the progenitors of the WDs in these systems because the timescale of the CE phase is very short and the M dwarfs usually have a deep surface convective zone. Another possible explanation for this behaviour is that the so-called high-logg problem is presented in 1D model atmosphere of DA WDs (Tremblay et al. 2013). In this work, the values of the effective temperature and surface gravity of the DA WDs (with $T_{\text{eff}} \lesssim 14,000$ K) determined in 1D models are revised to those in 3D model atmosphere for the DA WDs (Tremblay et al. 2013). Then, the average mass of the WDs in new WDMS binaries and in all WDMS ones identified by us is derived to be of $0.632M_{\odot}$ and $0.692M_{\odot}$, respectively. This is similar to the results recently derived by Kepler (2014).

The stellar parameter distributions have used to probe the general properties of the WDMS binaries, it is found in Fig. 2 that the effective temperature of the WDs in the majority of our WDMS binaries is lower than 25,000K, the

surface gravity of the WDs in WDMS binaries peaks at $\log g_{\text{WD}} \sim 8.0$, and the mass of them peaks at $\sim 0.5M_{\odot}$. As shown in Fig. 3, the cooling age of the WDs peaks at $\log \text{Age}_{\text{cool}} \sim 8.6$, the mean cooling age of the WDs is of $\sim 2.0 \times 10^8$ yrs, and the young WDs are very rare. Meanwhile, the spectral types of M-dwarfs are derived from their effective temperature through an empirical $\text{Sp} - T_{\text{eff}}$ relation (Rebassa-Mansergas et al. 2007). As seen from Fig. 4, the spectral types of most WDMS binaries are located in a region between M3 and M6. These results are consistent with the results derived by the previous investigators (e.g. Silvestri et al. 2006; Heller et al. 2009; Liu et al. 2012; Rebassa-Mansergas et al. 2007, 2012, 2013).

121 WDMS binaries are found to be observed by SDSS spectral survey several times. In these binaries, at least three such binaries (SDSS J220451.62+113230.8, SDSS J095043.96+391541.7 and SDSS J111544.56+425822.4) are recently discovered by us from SDSS DR9 and DR10, respectively. Four WDMS binaries, J095043.96+391541.7, SDSS J111544.56+425822.4, SDSS J143947.62-010606.9 (Silvestri et al. 2006), and SDSS J131751.72+673159.4 (listed in Rebassa-Mansergas et al. 2013) show hydrogen emission in all observable Balmer series lines in addition He I emission (see Fig. 6). A possible explanation for this behaviour is photoionization and recombination of M dwarfs caused by the irradiation of M dwarfs due to their very hot WD companions. It is found in Fig. 6 that the WDs in these WDMS binaries usually have a very high effec-

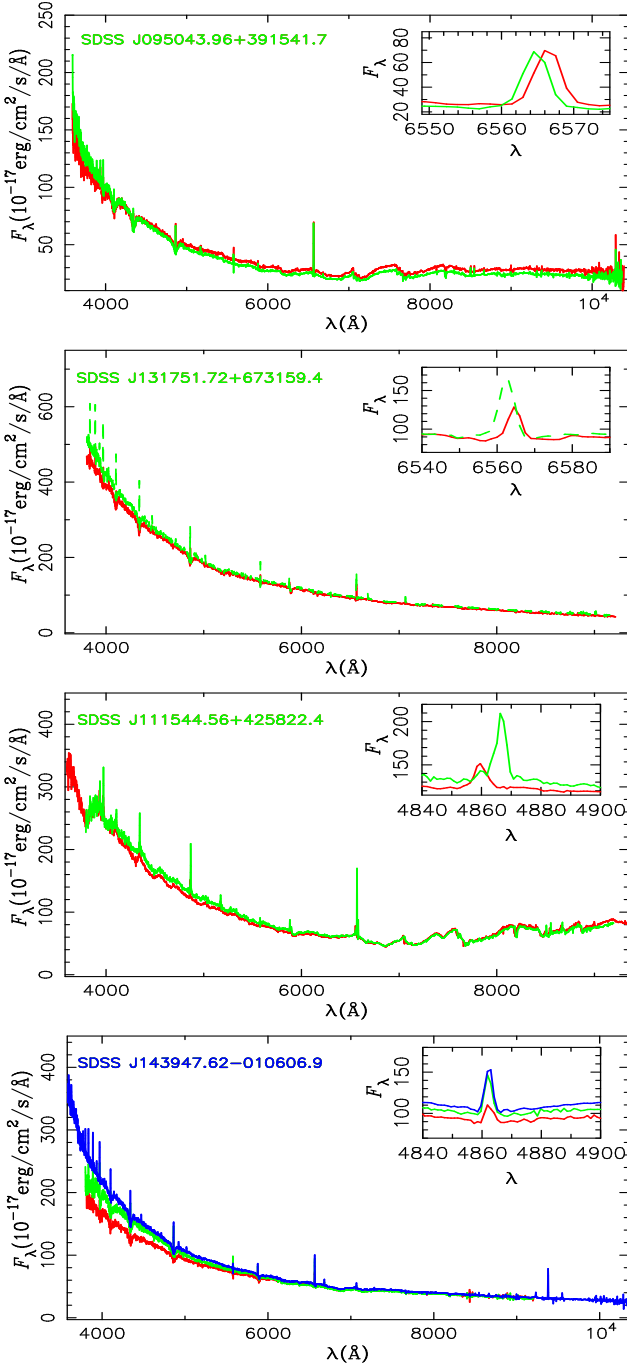


Figure 6. Shown is the spectra of four specific WDMS binaries with hydrogen line emission and Helium line emission. Top panel: the SDSS spectra of SDSS J095043.96+391541.7. The second panel: the spectra of SDSS J131751.72+673159.4 (listed in Rebassa-Mansergas et al. 2013). The third panel: the spectra of SDSS J111544.56+425822.4. Bottom panel: The spectra of SDSS J143947.62-010606.9 (Silvestri et al. 2006).

tive temperature, and therefore they should be very young WDs according to their spectral profile (such as SDSS J095043.96+391541.7 with $T_{\text{eff}} = 60,000$ K and $\log \text{Age} = 5.28$ and SDSS J111544.56+425822.4 with $T_{\text{eff}} = 40,000$ K and $\log \text{Age} = 7.71$). Also as seen from Fig. 6, three of these binaries show the shift of H_{α} or H_{β} emission line,

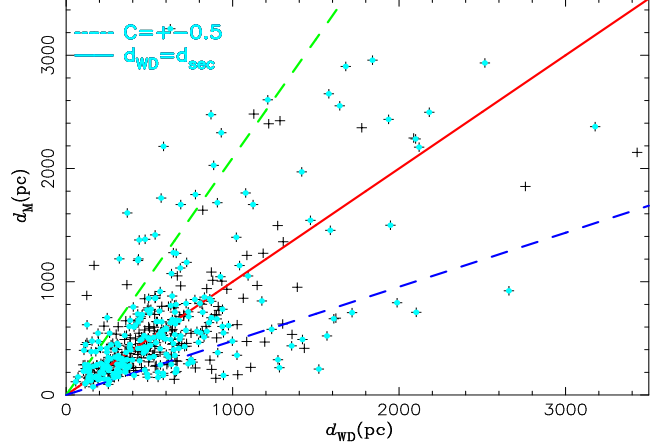


Figure 7. The distribution of the distances of the two components in WDMS binaries identified by us from SDSS. The solid line denotes the case with $d_{\text{WD}} = d_{\text{sec}}$, the blue dashed line denotes the case with $C = +0.5$ and the green dashed line represents the case with $C = -0.5$. The pluses represent all WDMS binaries (including new WDMS binaries and those found by Li et al. 2014), the solid dots represent those newly found from DR10, together with those containing a DB WD component identified by Li et al. (2014).

implying that the components of these binary systems exhibit the variation in their radial velocities, especially for the system SDSS J095043.96+391541.7, its two SDSS spectra only cover a time interval of one day (MJD55622 and MJD55623). This suggests that four such WDMS binaries should be PCEBs with a short orbital period, and the system SDSS J143947.62-010606.9 should be a PCEBs with very low orbital inclination. Since these young PCEBs are not polluted not only by mass transfer but also by angular momentum loss, they have a special significance for limiting the results of CE phase of the binary evolution. We will monitor the variation in the radial velocities of these binaries to obtain their orbital periods.

Two independent distances for two components in WDMS binaries are derived on the basis of two flux-scaling factors described in Heller et al. (2009). It is found in Fig. 7 that 80 per cent of the WDMS binaries with a DA/DB white dwarf and an M dwarf satisfy $d_{\text{WD}} \simeq d_{\text{sec}}$ (i.e. they locate in a range with $|C| < 0.5$). Approximately one-fifth of WDMS binary systems suffer a significant difference between d_{WD} and d_{sec} . This is similar to the results derived by Liu et al. (2012) and Rebassa-Mansergas et al. (2007). The significant difference between d_{WD} and d_{sec} might be a result of the H_{α} emission and/or other types of Balmer emission (such as SDSS J143012.51+250437.6, SDSS J213019.79+061204.6, and SDSS J215713.29-001958.8) owing to the stellar activity of the M dwarfs in these WDMS binaries, which might cause a too early spectral type to be determined for the M dwarfs in WDMS binaries (Heller et al. 2009; Rebassa-Mansergas et al. 2007; Silvestri et al. 2006). Meanwhile, another explanation for this behaviour is the expansion in the radii of M dwarfs irradiated by their close hotter WD primary (Silvestri et al. 2006; Heller et al. 2009), such as in SDSS J095043.96+391541.7 and SDSS J111544.56+425822.4 mentioned above.

ACKNOWLEDGEMENTS

This project was partly supported by the Chinese Natural Science Foundations (Grant Nos. 11373063, 11073049, 11273053, 11033008, 10821026, 11390374 and 2007CB15406) and Yunnan Foundation (Grant No. 2011CI053), and by the Chinese Academy of Sciences (KJCX2-YW-T24).

REFERENCES

- Abazajian K.N., Adelman-McCarthy J.K., Agüeros M.A., Allam S.S., Allende Prieto C., An D., Anderson K.S.J., Anderson S.F., 2009, *ApJS*, 182, 543
- Adelman-McCarthy J.K., Agüeros M.A., Allam S.S., et al., 2007, *ApJS*, 172, 634
- Adelman-McCarthy J.K., Agüeros M.A., Allam S.S., Allende Prieto C., Anderson K.S.J., Anderson S.F., Annis J., Bahcall N.A., et al., 2008, *ApJS*, 175, 297
- Althaus L.G., Benvenuto O.G., 1997, *ApJ*, 477, 313
- Baraffe I., Chantier G., Allard F., Hauschildt P.H., 1998, *A&A*, 337, 403
- Bergeron P., Wesemmel F., Beauchamp A., 1995, *PASP*, 107, 1047
- Davis P.J., Kolb U., Willems B., Gänsicke B.T., 2008, *MNRAS*, 389, 1563
- Dye S. et al., 2006, *MNRAS*, 372, 1227
- Heller R., Homeier D., Dreizler S., Østensen R., 2009, *A&A*, 496, 191
- Hjellming M.S., 1989, PhD thesis, AA (Illinois Univ. at Urbana-Champaign Savoy)
- Holberg J.B., Oswalt T.D., Barstow M.A., 2012, *AJ*, 143, 68
- Hurley J.R., Pols O.R., Tuot C.A., 2002, *MNRAS*, 329, 897
- Iben I.J., Livio M., 1993, *PASP*, 105, 1373
- Iben I.J., Tutukov A.V., 1986, *ApJ*, 311, 742
- Kepler S.O., Pelisoli I., Koester D., Ourique G., et al., 2014, *MNRAS*, accepted
- Koester D., 2010, *Mem. S. A. It.*, 81, 921
- Lawrence A., 2007, *MNRAS*, 379, 1599
- Lejeune T., Cuisinier F., Buser R., 1997, *A&AS*, 125, 229
- Lejeune T., Cuisinier F., Buser R., 1998, *A&AS*, 130, 65
- Li L.F., Zhang F.H., Han Q.W., Kong X.Y., Gong X.B., 2014, *MNRAS*, 445, 1331
- Liu C., Li L., Zhang F., Zhang Y., Jiang D., Liu J., 2012, *MNRAS*, 424, 1841
- Maxted P.F.L., Gänsicke B.T., Burleigh M.R., Southworth J., Marsh T.R., Napiwotzki R., Nelemans G., Wood P.L., 2009, *MNRAS*, 400, 2012
- Nebot Gómez-Morán A., Gänsicke B.T., Schreiber M.R., Rebassa-Mansergas A., Schwöpe A.D., Southworth J., Aungwerojwit A., Bothe M., Davis P.J. et al., 2011, *A&A*, 536, 43
- Paczynski, B., 1976, in *IAU Symp. 73: Structure and Evolution of Close Binaries*, 75
- Politano M., van der Sluis M., Taam R.E., Willems B., 2010, *ApJ*, 720, 1752
- Postnov K.A., Yungelson L.R., 2006, *Living Rev. Relativ.* 9, 6
- Raymond S.N., Szkody P., Hawley S.L., et al., 2003, *AJ*, 125, 2621
- Rebassa-Mansergas A., Gänsicke B.T., Rodríguez-Gil P., Schreiber M.R., Koester D., 2007, *MNRAS*, 382, 1377
- Rebassa-Mansergas A., Gänsicke B.T., Schreiber M.R., Koester D., Rodríguez-Gil P., 2010, *MNRAS*, 402, 620
- Rebassa-Mansergas A., Nebot Gómez-Morán A., Schreiber M.R., Gänsicke B.T., Schwöpe A., Gallardo J., Koester D., 2012, *MNRAS*, 419, 806
- Rebassa-Mansergas A., Agurto-Gangas C., Schreiber M.R., Gänsicke B.T., Koester D., 2013, *MNRAS*, 433, 3398
- Ren J.J., Luo A.L., Li Y.B., Wei P., et al., 2013, *AJ*, 146, 82
- Schreiber M.R., Gänsicke B.T., 2003, *A&A*, 406, 305
- Silvestri N.M., Hawley S.L., West A.A., Szkody P., Bochanski J.J., Eisenstein D.J., McGehee P., Schmidt G.D., et al., 2006, *AJ*, 131, 1674
- Silvestri N.M., Lemagie M.P., Hawley S.L., West A.A., Schmidt G.D., Liebert J., Szkody P., Mannikko L. et al., 2007, *AJ*, 134, 741
- Skrutskie M.F., 2006, *AJ*, 131, 1163
- Stoughton C., Lupton R.H., Bernardi M., Blanton M.R., Burles S., Castander F.J., Connolly A.J., Eisenstein D.J., et al. 2002, *AJ*, 123, 485
- Taam R.E., Sandquist E.L., 2000, *ARA&A*, 38, 113
- Taam R.E., Ricker P.M., 2010, *NewAR*, 54, 65
- Tremblay P.E., Ludwig R.G., Steffen M., Freytag B., 2013, *A&A*, 559, A104
- Warren S.J., et al., 2007, *MNRAS*, 375, 213
- Webbink R.F., 1984, *ApJ*, 277, 355
- Webbink R.F., 2008, in Milone E.F., Leady D.A., Hobill D.W., eds, *Astrophys. Space Sci. Libr. Vol. 352, Short-Period Binary Stars: Observations, Analyses, and Results*, Springer, Berlin, p. 233
- Wei P., Luo A.L., Li Y.B., Pan J.C., Tu L.P., Jiang B., Kong X., Shi Z.X., et al., 2012, *MNRAS*, 431, 1800
- Wright E.L., 2010, *AJ*, 140, 1868
- York D.G., Adelman J., Anderson J.E.Jr., Anderson S.F., Annis J., Bahcall N.A., Bakken J.A., Barkhouser R., et al., 2000, *AJ*, 120, 1579
- Zorotovic M., Schreiber M.R., Gänsicke B.T., 2011, *A&A*, 536, 42

This paper has been typeset from a \LaTeX file prepared by the author.